Published in final edited form as:

Adv Healthc Mater. 2023 October ; 12(26): e2300942. doi:10.1002/adhm.202300942.

Rapid and facile light-based approach to fabricate protease-degradable poly(ethylene glycol)-norbornene microgels for cell encapsulation

Ana Mora-Boza[a,b,c,†], **Saron G. Ghebrezadik**[b,d,†], **Johannes E. Leisen**[b], **Andrés J. García**[a,b,*]

[a]Woodruff School of Mechanical Engineering, Georgia Institute of Technology, Atlanta GA, USA

[b]Petit Institute for Bioengineering and Bioscience; Georgia Institute of Technology, Atlanta GA, USA

[c]CÚRAM, University of Galway, Ireland

[d]Agnes Scott College, Decatur GA, USA

Abstract

Thiol-norbornene photoclickable PEG-based (PEG-NB) hydrogels are attractive biomaterials for cell encapsulation, drug delivery, and regenerative medicine applications. Although many crosslinking strategies and chemistries have been developed for PEG-NB bulk hydrogels, fabrication approaches of PEG-NB microgels have not been extensively explored. Here, we present a fabrication strategy for 4-arm amide-linked PEG-NB (PEG-4aNB) microgels using flow-focusing microfluidics for human mesenchymal stem/stromal cell (hMSCs) encapsulation. PEG-4aNB photochemistry allowed high-throughput, ultra-fast generation, and cost-effective synthesis of monodispersed microgels (diameter 340 ± 18, 380 ± 24, and 420 ± 15 μm, for 6, 8, and 10 wt% of PEG-4aNB, respectively) using an *in situ* crosslinking methodology in a microfluidic device. PEG-4aNB microgels showed *in vitro* degradability due to the incorporation of a protease-degradable peptide during photocrosslinking and encapsulated cells showed excellent viability and metabolic activity for at least 13 days of culture. Furthermore, the secretory profile (i.e., MMP-13, ICAM-1, PD-L1, CXCL9, CCL3/MIP-1, IL-6, IL-12, IL-17E, TNF-α, CCL2/MCP-1) of encapsulated hMSCs showed increased expression in response to IFN-γ stimulation. Collectively, this work shows a versatile and facile approach for the fabrication of protease-degradable PEG-4aNB microgels for cell encapsulation.

Graphical Abstract

Monodispersed PEG-NB microgels are fabricated using an ultra-fast generation and cost-effective *in situ* crosslinking methodology in a microfluidic device. PEG-NB microgels are synthetized by varying the initial macromer concentration (6, 8 and 10 wt%), and incorporating a protease-cleavable crosslinking peptide, which provides degradation properties to the microgels. The

*Corresponding author.
†These authors contributed equally to this work

Conflict of Interest
The authors declare no conflict of interest.

methodology allows human mesenchymal stem/stromal cells (hMSCs) encapsulation with high viability and functionality (e.g., secretory activities).

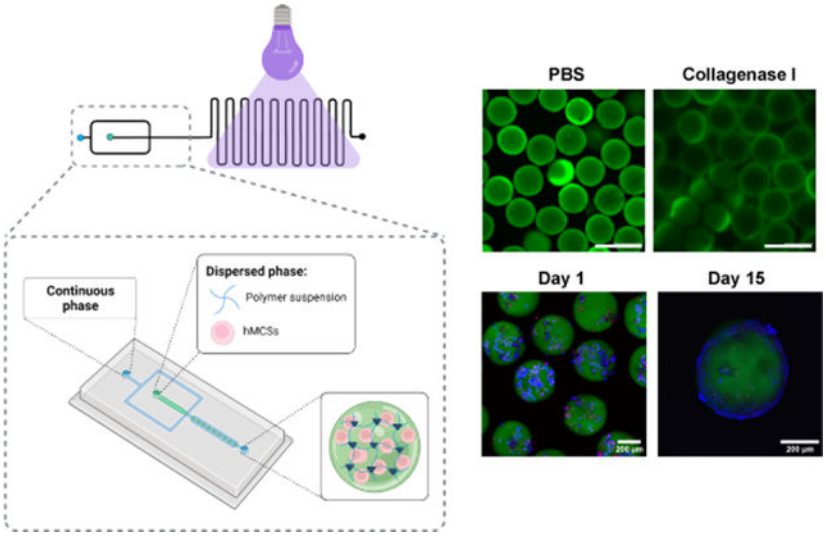

Keywords

Microgels; PEG-norbornene; photopolymerization; microfluidics; mesenchymal stem/stromal cells

1. Introduction

Hydrogel microparticles, or microgels, have emerged as versatile biomaterial platforms for diverse biomedical applications due to their modularity, injectability (i.e., delivery via minimally invasive techniques), and enhanced integration with host tissue. [1] Various microgel fabrication strategies for cell encapsulation have been investigated using natural and synthetic polymers,[1c] including microfluidic-based routes that allow high-throughput production of monodispersed microparticles.[1a] The synthesis of poly(ethylene glycol) (PEG)-based microgels using microfluidic technology has been explored for cell encapsulation and drug delivery applications[1a, 2] due to the ability of this synthetic chemistry to decouple biochemical, physical, and mechanical properties, enabling tunability of critical network parameters and a highly controlled cellular microenvironment. In recent years, thiol-norbornene (thiol-ene) photoclickable PEG-based macromers have gained special attraction for the fabrication of hydrogel microparticles for drug delivery and cell encapsulation applications.[3] PEG-norbornene (PEG-NB) photochemistry provides several advantages in comparison to other photocrosslinking methodologies based on vinyl- or methacrylated macromers, such as PEG-acrylate or PEG-methacrylate.[3a] PEG-NB gelation reaction occurs at stoichiometric ratios and physiological pH with a low concentration of radicals during crosslinking, which reduces the cytotoxicity derived from the presence of free radicals and unreacted components compared to chain-growth polymerization processes. In addition, the degree of network homogeneity of crosslinked PEG-NB gels is high in comparison to random chain-growth crosslinking reaction because of the absence of homopolymerization between norbornene groups. This fact, together with the high

stoichiometric control of the reaction, permits facile incorporation of cysteine-containing peptides or thiolated ligands via photoconjugation to the polymer backbone. Moreover, and importantly, PEG-NB photochemistry is less sensitive to oxygen inhibition, which increases its efficiency and gelation kinetics several orders of magnitude in comparison to acrylate-based chain growth photopolymerization (e.g., polyethylene glycol diacrylate (PEGDA)).[3a, 3c] As such, PEG-NB photopolymerization is an attractive mechanism to produce microgels for cell encapsulation, especially using microfluidic technologies due to the fast crosslinking conditions. PEG-NB microgel synthesis has been reported using different biofabrication techniques [2c, 4] for several biomedical applications, [1c, 3b, 3c, 4d, 5] including cell microencapsulation. [3c, 4c, 5b] For example, Xin and coworkers [4b] fabricated PEG-NB microgels that could be assembled into 3D scaffolds to encapsulate hMSCs. Microgels were fabricated using electrospraying technique and the scaffolds showed a 3D permissive environment due to microporosity that provided a means to regulate cell spreading and mechanosensing. In other work, [4a] they applied the electrosprayed PEG microspheres as ink for 3D printing of building blocks. Another study [5b] explored the use of dithiol crosslinkers with different lengths for the fabrication of PEG-NB microspheres with different shapes to encapsulate 3T3 fibroblasts. They demonstrated that the crosslinker length offers a versatile approach to tune hydrogel dynamics. Although flow-focusing microfluidics has been explored for the fabrication of PEG-NB microparticles, these fabrication protocols are based on crosslinking of the microparticles after collection, which can lead to higher polydispersity and makes necessary the use of sophisticated and expensive continuous phases (e.g. fluorocarbon-based oils) in the microfluidic device to prevent microparticles from merging during collection when they are not fully crosslinked. [3c, 4c, 4e, 5b, 6] Moreover, these oils are extremely difficult to remove. In this study, we describe the synthesis of PEG-NB based microgels using an *in situ* crosslinking approach that allows the high-throughput and ultra-fast production of monodisperse protease-degradable microgels in a flow-focusing microfluidic device for cell encapsulation.

Degradable microgels containing encapsulated cells are of special interest because the material persistence and mechanical properties will play a key role on the host tissue-encapsulated cell crosstalk and immune-related processes after implantation. [2b] Whereas degradable PEG-NB bulk hydrogels have been previously investigated, [7] this modality has barely translated to microgels fabricated through microfluidics-based polymerization. Jiang et al. [4c] developed dissolvable PEG-NB microgels using a fast-degrading macromer poly(ethylene glycol)-norbornene-dopamine (PEGNB-Dopa) to fabricate microporous scaffolds containing hMSCs. The microgels could be used as sacrificial porogens since they rapidly dissolved upon contacting with an aqueous solution, provided an excellent method to fabricate cell-laden macroporous hydrogels. However, recent efforts have focused on microgels with tunable degradability.[2b, 4c, 5a, 8] In our group, different linkages of ester and amide groups within thiol-ene groups of PEG-NB were examined to improve *in vivo* hydrogel stability.[7a] The *in vitro* and *in vivo* degradation of 4-arm ester-linked PEG-NB (PEG-4eNB) macromer-based hydrogels was compared to 4-arm amide-linked PEG-NB (PEG-4aNB) macromer-based gels, and we showed that replacement of the ester linkage for an amide group significantly mitigates the rapid *in vivo* degradation of PEG-4eNB hydrogels but maintains equivalent mechanical and crosslinking properties.

Moreover, PEG-4aNB showed high cytocompatibility for encapsulated human mesenchymal stem/stromal cells (hMSCs) and rat islets, indicating their suitability as biomaterial platform for cell encapsulation applications. Herein, we present a synthesis strategy based on flow-focusing microfluidics for the generation of monodispersed PEG-4aNB microgels for hMSC encapsulation. Moreover, we explored the incorporation of a protease-degradable peptide in the PEG-4aNB microgel backbone to provide microgels with a precise control over degradation rates, in contrast to previously reported degradable PEG-NB microgels, whose hydrolytic degradation occurs in 2 h upon contact with buffer solution.[4c] We demonstrate that monodispersed protease-degradable microgels can be fabricated using *in situ* crosslinking approaches in a high-throughput and rapid manner without the need of expensive continuous phases. Three different PEG-4aNB macromer concentrations (6, 8 and 10 wt%) were analyzed for microgel fabrication and hMSC encapsulation. PEG-4aNB microgels showed controlled *in vitro* degradability in presence of collagenase I, and this approach is compatible with hMSCs encapsulation with sustained cell viability and increased metabolic activity over 15 days. Additionally, we investigated the secretory profile of encapsulated hMSCs in the microgels for 23 different analytes upon stimulation with interferon-gamma (IFN-γ) and observed significant cytokine upregulation, indicating the immunoregulatory potential of the encapsulated cells in PEG-4aNB microgels.

2. Experimental Section

2.1 Microfluidics Device Fabrication

PDMS microfluidic devices were prepared as previously reported [9]. Briefly, PDMS was cast using soft lithography and SU8 masters with microfluidic device patterns and heated to 110 °C for 20 min. The resulting PDMS microfluidic devices were removed from the wafer, bonded to glass slides, and heated overnight to 70 °C.

2.2 PEG-4aNB Microgel Fabrication

Microgels were fabricated using a flow-focusing microfluidic device with a 300 μm nozzle containing a serpentine channel at the outlet (Figure 1). Three PEG-a4NB macromer (20 kDa, Jenkem Technologies) concentrations (6, 8 and 10 %wt) were evaluated for the formation of microgels. PEG-a4NB was conjugated to thiol-PEG-FITC (1.0 mM, 1 kDa, Nanocs) to facilitate microgel visualization and characterization. The aqueous phase consisted of a polymer solution of PEG-4aNB, 2.0 mM of RGD (GRGDSPC, Vivitide) as adhesive ligand, VPM (protease-degradable peptide at 4.2, 6.1, and 8.0 mM for 6, 8, and 10 wt% of PEG-4aNB, respectively, GCRDVPMSMRGGDRCG, Genscript) as crosslinker peptide, and 3.0 mM of lithium phenyl-2,4,6-trimethylbenzoylphosphinate (LAP) as photoinitiator agent. These reagents were dissolved in 10 mM HEPES in PBS. The continuous phase consisted of mineral oil (Sigma) with 2% SPAN80 (Sigma). Polymer droplets were crosslinked using UV light (OmniCure S2000 Spot UV Curing System equipped with a 365 nm filter and a collimator, Excellitas Technologies) at an intensity of 32 mW/cm^2 in the serpentine channel of the device (*in situ* approach) or after collection in a 15 mL Falcon tube. Flow rates for aqueous and continuous phase were adjusted to 18 μL/min and 33 μL/min, respectively. Microgels were washed four times after collection to remove continuous phase using cell strainers (40 μm nylon mesh, PluriStrainer®) and

centrifuged at 350g for 5 min. Post collection irradiated microgels were used as comparison for quality control of the *in situ* microgel fabrication protocol.

2.3 Microgel Characterization

Microgel size distributions for each macromer concentration and methodology were analyzed using a Biotek Cytation 3 spectrophotometer after fabrication and purification. Fluorescence images of the microgels were acquired with Biotek Cytation software through its “Read Image” function with a 1.25X objective and GFP 469/525 nm filter cube. Droplet diameter was measured using the cellular analysis plug-in in the Cytation Gen Software as previously described.[2b] Microgel samples for *in situ* and post-collection approaches were placed in a Greiner Bio-One SensoPlate™ 24 Well Flat-Bottomed microplate with lid. The diameter of at least 100 microgels for each microgel composition and approach was recorded. Collected data is from a minimum of three independent runs per approach. For microgel degradation analysis, microgels were incubated in 3.9 units/mL collagenase I solution in PBS at 37 °C. For qualitative degradation evaluation, images of the microgels were taken via confocal microscopy after 1 hour and 5 days of incubation. Quantitative degradation of ~220 microgels for each microgel composition in PBS (control) and collagenase I solution was evaluated by tracking the fluorescence signal of FITC release at 1 h, 1 and 5 days of incubation at 37 °C. Microgels were placed in 24 trans-well plates and collagenase solutions or PBS were added to the well (n = 3 per group and condition). The fluorescence signal was measured using the BioTek Synergy H4 microplate reader after transferring 100 μL of the microgel degradation solution to a black-opaque Costar® 96 well-plate. Final fluorescence was calculated by subtracting the fluorescence value of the control (PBS) to the collagenase I sample per time and microgel composition.

Microgel crosslinking density was evaluated for 8 wt% composition using diffusion nuclear magnetic resonance (NMR).[10] Data were recorded using a Bruker AV3 NMR spectrometer operating at a ^{1}H frequency of 400 MHz using the Diff50 Diffusion Accessory. The Stimulated Echo sequence was used with a delay $\Delta = 20$ ms between gradients with a duration of $\delta = 1$ ms. Spectra were recorded for a total of 64 gradient steps varying linearly to values up to 1500 G/cm. The decay of spectral densities in the NMR spectrum measured as a function of the gradient strength was used to determine the Brownian self diffusion (i.e., translational motion) of individual moieties such as water or the polymer. The samples for this study were *in situ* crosslinked PEG-4aNB microgels for 8 wt% composition (prepared as described in section 2.2) and PEG-4aNB hydrogels with the same composition prepared and crosslinked using the same parameters for comparison.

2.4 Cell Encapsulation

hMSCs were obtained from the Institute for Texas A&M Health Science Center College of Medicine Institute for Regenerative Medicine at Scott & White. The hMSCs were harvested from the bone marrow of a 24-year-old healthy male donor under IRB-approved protocols (donor number 8801).[11] Cells showed positive expression (>95%) for CD90, CD105, CD73a and negative (<2%) for CD34, CD19, CD11b, CD45, CD79a, HLA-II, CD14, and were confirmed *Mycoplasma sp* negative. Cells were cultured in α-Minimum Essential medium (α-MEM, ThermoFisher/GIBCO) containing fetal bovine serum (FBS,

16.5%, ThermoFisher/GIBCO), L-glutamine (2 mM, ThermoFisher/GIBCO), penicillin (100 units/mL, ThermoFisher) and streptomycin (100 μg/mL, ThermoFisher). Cells were maintained at 37 °C and CO_2 (5%) and subcultured at 70–80% confluence. Cells at passages 2–5 were used for all experiments. For cell encapsulation in microgels, cells were trypsinized, pelleted by centrifugation, and resuspended in polymer mix solution at a final density of 1.2×10^6 cells/mL. Synthesis of microgels containing hMSCs was performed as described in section 2.2, but the encapsulated cells in the microgels were washed with media to remove the continuous phase.

2.5 hMSC Viability and Metabolic Activity

PEG-4aNB microgels with encapsulated hMSCs were statically cultured for 15 days in complete α-MEM, which was replaced with fresh media every 3 days. At selected time points, microencapsulated cells were removed from culture and stained for 15 min with BioTracker 405 Blue Mitochondria dye at final concentration of 1 μM for live cells (Sigma) and TOTO™−3 Iodide dye at final concentration of 1 μM for dead cells (Thermofisher) to analyze cell viability. At least 200 cells were imaged at each time point using confocal microscopy (Zeiss LSM 710). Viability over time was calculated by taking the ratio of live cells to total cells (mean ± standard deviation). Metabolic activity of the encapsulated cells over time was evaluated using the alamarBlue™ reagent (Invitrogen). Microgels containing hMSCs were cultured in 24 trans-well plates for 13 days. At selected time points (1, 4, 7 and 13 days), culture media was replaced by 10% v/v solution of alamarBlue™ in α-MEM. After 4 h of incubation at 37 °C, alamarBlue™ solution was collected and replaced by α-MEM, and alamarBlue™ fluorescence of each sample extract was measured at 525/590 nm (excitation/emission) in a BioTek Synergy H4 microplate reader.

2.6 Paracrine Secretory Profile Analysis

Paracrine factor secretion for hMSCs encapsulated in PEG-4aNB microgels was evaluated under the presence of interferon-γ (IFN-γ) as a stimulant. An average of 128 microgels containing hMSCs per group were cultured overnight in α-MEM in 24 trans-well plates, then the media was replaced by α-MEM solution containing IFN-γ at a final concentration of 50 ng/mL, and the encapsulated cells were cultured for 24 h. Cell supernatant was collected and centrifuged at 14,000g for 20 min at 4 °C. Samples were analyzed for 23 analytes using a custom Luminex® Assay (R&D Systems) following the manufacturer's instructions. Secretory factor expression for hMSCs encapsulated in PEG-4aNB microgels was analyzed by hierarchal clustering, multivariate discriminant analysis, and correlation clusters using JMP Pro 15 (JMP Software from SAS; Cary, NC). Hierarchal clustering used Ward Method clustering method, with data standardized by analyte.

2.7 Statistical Analysis

Statistical analyses were performed using GraphPad Prism 8 (Graph-Pad Software Inc., La Jolla, CA). For cell viability and alamarBlue™ assays, two-way ANOVA was performed to study significant differences in cell viability percentages and metabolic activity among samples. For individual cytokine data, one-way ANOVA was used to find significant differences among samples. All data represented as mean ± standard deviation (SD).

3. Results

3.1. PEG-4aNB Microgels Synthesis and Characterization

Photopolymerizable PEG-4aNB[7a] was used for the fabrication of hydrogel microparticles (i.e., microgels) using flow-focusing microfluidics. PEG-4aNB macromer was functionalized via Michael type addition with a linear thiol-PEG-FITC molecule for microgel tracking and RGD peptide as adhesive ligand. Figure 1a describes the PEG-4aNB photopolymerization reaction applied for microgel generation in the microfluidic device using VPM as protease degradable crosslinker and LAP as photoinitiator. PEG-4aNB degradable microgels were fabricated using a flow-focusing microfluidic device with a serpentine channel segment at the outlet (Figure 1b). Aqueous solution, containing the functionalized macromer at different polymer concentrations (6, 8, and 10 wt%), crosslinking agent, and photoinitiator, was pumped into the microfluidic device through one of the independent inlets and focused to the continuous phase to allow water/oil emulsion and droplet generation. Once microdroplets were generated, they flowed through the serpentine channel and were either: (i) directly irradiated with UV light inside the device (i.e., *in situ* crosslinking); or (ii) irradiated with UV light after collection (i.e., post-collection crosslinking). For the first approach, the serpentine channel was essential to increase residence time of the microgels in the device and ensure microparticle crosslinking.

In situ crosslinked microgels showed more uniform size distributions for every polymer formulation in comparison to post-collection crosslinked microgels (Figure 2a). *In situ* crosslinked microgels for every polymer concentration showed homogeneous, round morphologies with low coefficients of variation (CV<6%) in size compared to microgels crosslinked after collection, which showed %CV values >35% (Figure 2b). Remarkably, *in situ* crosslinked microgels showed CV values of 5%, 6%, and 3%, for 6, 8 and 10 wt%, respectively, demonstrating the efficacy of the *in situ* crosslinking methodology to obtain PEG-4aNB microparticles with tight size distributions. For the *in situ* crosslinking approach, flow rates of aqueous and continuous phases were optimized to prevent the formation of pre-crosslinked hydrogel particles that could clog the device. Thus, high flow rates (18 μL/min and 33 μL/min, for aqueous and continuous phases, respectively) were used, which also provided a high-speed methodology for microgels fabrication (260 ± 35 microgels/min), being able to run 100 μL of polymer solution in ~5 min. PEG-4aNB microgels synthesized via *in situ* crosslinking showed an increasing average size as the macromer concentration increased, obtaining diameter values of 340 ± 18, 380 ± 24, and 420 ± 15 μm for 6, 8 and 10 wt%, respectively. These values correlated well with the nozzle size of the microfluidic device (300 μm), showing a slightly larger size after purification and incubation in PBS probably due to swelling, an effect that was more evident for 10 wt% formulation. PEG-4aNB microgels crosslinked after collection showed higher diameter values in comparison to *in situ* crosslinked microgels with very high standard deviation values, 520 ± 200, 670 ± 460 and 590 ± 210 μm for 6, 8 and 10 wt%, respectively. These results demonstrate that *in situ* crosslinking of microgels in the microfluidic device is a better methodology to fabricate homogeneous and monodisperse PEG-4aNB microgels in comparison to traditional post-collection crosslinking approaches. Crosslinking degree for *in situ* crosslinked PEG-4aNB microgels was evaluated using diffusion NMR (Figure

S1). 8 wt% microgel composition was compared to 8 wt% PEG-4aNB bulk hydrogels fabricated under the same experimental conditions. Translational motion in a crosslinked polymer network will exhibit restricted length scales, which are well below the length scale associated with the spatial distribution of crosslinks, which is in the sub-μm range. In fact, no significant decay was observed for the stimulated echo of the polymer chains of the microgel and the hydrogel even at the highest achievable gradient strength. This indicates the absence of translational motion below the detection limit of the experiment ($D < 5 \times 10^{-13}$ m^2/s corresponding to a mean-square displacement below 0.1 μm during the selected time interval of $\Delta = 20$ ms). For comparison, significant Brownian diffusion could be measured for the non-crosslinked polymer solution ($D = 1.64 \times 10^{-11}$ m^2/s, corresponding to a measurable mean square displacement of 0.8 μm).

Proteolytic degradation of PEG-4aNB microgels in the presence of collagenase I was assessed by tracking the amount of PEG-FITC released into solution. Since PEG-FITC is covalently linked to the PEG-4aNB macromer, its release is indicative of the degradation of the polymer network.[2b] PEG-FITC release significantly increased over time for every polymer concentration in the presence of collagenase I (Figure 2c), confirming that microgels can be proteolytically degraded. No significant differences were found between microgel compositions after 1 hour and 1 day of incubation, whereas significant differences were observed for longer times (i.e., 5 days) for 6 and 8 wt% when compared 10 wt% microgels. Microgel degradation was confirmed by fluorescence microscopy, showing no microgels present after 5 days of incubation in collagenase I. In contrast, microgels incubated in PBS (negative control) did not show morphological changes, maintaining their round and homogeneous shape over time (Figure 2d).

3.2. Cell Encapsulation In PEG-4aNB Microgels Using *In Situ* Crosslinking Approach

The *in situ* crosslinking approach was evaluated for encapsulation of hMSCs in PEG-4aNB microgels. A hMSCs suspension was mixed with the functionalized macromer solution and pumped into the device as previously described. Cells were successfully encapsulated in PEG-4aNB microgels and confocal images of live/dead staining for encapsulated cells showed high cell viability over 15 days of culture for every microgel composition (Figure 3a,b). After 3 days of culture, encapsulated hMSCs proliferated and started to colonize the microgel surface, showing a spread morphology. After 15 days of culture, encapsulated hMCSs had colonized the whole microgel surface (Figure 3a). Quantitative analysis of encapsulated hMSCs viability indicated that cell viability was slightly reduced after microgel encapsulation in comparison to initial hMSCs viability after trypsinization (84±2%), which is attributed to handling during washing steps and direct UV irradiation during *in situ* crosslinking. Nevertheless, cell viability was maintained over time for 8 and 10 wt% microgels (Figure 3b). A significant decrease of cell viability was observed for encapsulated hMSCs in 6 wt% microgels after 13 days of culture, which might be due to softer matrix obtained for this formulation compared to 8 and 10 wt% microgels.

Metabolic activity of encapsulated cells was analyzed by alamarBlue assay (Figure 3c), showing increasing fluorescence signals over time for every microgel formulation. These results indicate that encapsulated hMSCs exhibited metabolic activity over time that was

positively correlated to the increasing macromer concentration in the PEG-4aNB microgels, with higher metabolic activity for hMSCs encapsulated in 10 wt% microgels, followed by 8 and 6 wt%, respectively.

3.3. Multiplex Secretome Analysis of Encapsulated MSCs in PEG-4aNB Microgels

Analytes secreted by hMSCs (i.e., secretome) exert powerful therapeutic actions on tissue regeneration processes,[12] and some of them have also been proposed as surrogate potency markers of hMSCs.[11, 13] To assess the secretome profile of encapsulated hMSCs in PEG-4aNB microgels, we performed a 23-plex analyte panel assay by stimulating the cells with IFN-γ. Figure 4a shows the heat map and two-way hierarchal clustering analysis of analyte secretion in presence and absence of IFN-γ for 6, 8 and 10% microgel formulations. As expected, hMSCs cultured in presence of IFN-γ showed a higher secretion of the evaluated analytes for all microgel compositions, confirming their stimulation via IFN-γ. Significant differences are observed for 10 wt% microgel concentration, which had the lowest analytes secretion in absence of IFN-γ, but were significantly upregulated upon IFN-γ stimulation. Figure 4c shows the individual analysis for secreted analytes that showed statistical differences after IFN-γ stimulation for the different PEG-aNB concentrations. Among all analytes, programmed cell death protein 1 (PD-L1), matrix metalloproteinase 13 (MMP-13), intercellular adhesion molecule 1 (ICAM-1), and chemokine ligand 2 or monocyte chemoattractant protein 1 (CCL2/MCP-1) were significantly higher for every microgel formulation in the presence of IFN-γ. MMP-13 plays a key role in the breakdown of cartilage and progression of osteoarthritis through the cleavage of collagen II, being a promising target for the treatment of the disease.[14] ICAM-1 is a cell surface glycoprotein and an adhesion receptor that is best known for regulating leukocyte recruitment from circulation to inflammation sites, being recognized as a key regulator of many essential tissue functions.[15] Among analytes that were only significantly upregulated in 10 wt% PEG-4aNB microgels, we found macrophage inflammatory protein-1 alpha (CCL3/MIP-1), three interleukin cytokines (interleukin-6 (IL-6), interleukin-12 (IL-12), and interleukin-25, also known as IL-17E), and tumor necrosis factor alpha (TNF-α). The family of IL-6 and IL-12 plays critical roles in different immune responses.[16] For its part, IL-17E is a unique cytokine of the IL-17 family that triggers the expression of type 2 immunity-related cytokines.[17] Finally, chemokine ligand 9 (CXCL9) was significantly upregulated in the 8 and 10 wt% microgel formulation. CXCL9 is an important immunoregulatory factor that acts as a T-cell chemoattractant and regulates PD-L1 in several types of cancer.[18]

4. Discussion

Thiol-norbornene (thiol-ene) photoclickable PEG-based hydrogels are versatile biomaterials for tissue engineering and regenerative medicine applications.[3a, 3c, 7a] Its unique photopolymerization reaction provides several advantages when compared to other photocrosslinkable polymers like vinyl- or methacrylate-based macromers (e.g., PEG-acrylate, PEG-methacrylate). Among the main advantages, we highlight that (i) PEG-NB reaction takes place in physiological conditions and does not need high radical concentration during the initiation step compared with chain-growth polymerization reactions; (ii) the gelation reaction occurs in a stoichiometric ratio, which minimizes the chemical

toxicity due to the reduced presence of unreacted components; and (iii) the step-growth photopolymerization process is less sensitive to oxygen inhibition compared to other acrylate-based polymers such as PEGDA. [2c, 3a, 3c] These properties render the PEG-NB crosslinking reaction a fast and highly cytocompatible methodology in comparison to acrylated-based traditional photopolymerization processes.[3a] Therefore, we present a rapid and facile microfluidic technique for the fabrication of PEG-NB microgels for cell encapsulation. Microfluidics fabrication of PEG-NB microgels has been previously explored using fluorocarbon or silicone-based oils as continuous phases to avoid microparticle merging during collection.[3c, 4c, 4e, 5b, 6] The selection of an optimal continuous phase for droplet-based microfluidic generation of microgels plays a key role in the high-throughput generation of highly monodisperse microparticles[19]. The use of these sophisticated oils as continuous phases not only makes the fabrication process orders of magnitude more expensive, but also technically more complicated, since they are difficult to remove from the aqueous phase during microgel purification. [3c] In this study, we compared *in situ* and post-collection crosslinking approaches using a flow-focusing microfluidic device for microgel generation (Figure 1), and we demonstrated that *in situ* irradiation of the polymer droplets in the device led to monodispersed microparticles only using the traditional and cost-effective mineral oil/SPAN80 mixture as a continuous phase (Figure 2). To the best of our knowledge, none of the published protocols for the generation of PEG-NB microgels is based on the use mineral oil as a continuous phase. With this microgel fabrication approach, we were able to tune the microgel formulation by changing the macromer concentration from 6 to 10 wt% and obtained homogeneous microparticles for the 3 different PEG-4aNB microgel groups. In addition, microgel sizes for all 3 formulations fabricated with the *in situ* crosslinked approach showed similar diameter when compared to the nozzle size of the microfluidic device, as opposed to PEG-4aNB microgels crosslinked after collection. This aspect would facilitate the modulation of the microgel size by simply modifying the nozzle size of the microfluidic device, as we have previously shown for maleimide-functionalized PEG macromers.[1a] One of the main advantages of using microfluidic techniques is the high-throughput generation of homogeneous microparticles in a short amount of time, but high-throughput fabrication is not always directly related to high speed generation. Our *in situ* crosslinking approach provides a rapid and high-throughput protocol for microgels synthesis using a high flow rate (18 μL/min for polymer phase) that allows to run 100 μL of polymer solution in 5 min, being significantly faster in comparison to other microfluidic techniques reported for microgel fabrication.[1a, 3c] Due to the lack of homopolymerization between norbornene groups of the macromer and the orthogonal reactivity between norbornene and thiol group,[3a] PEG-NB crosslinking reaction allows the photoconjugation of cysteine containing peptides or thiolated proteins to modify the polymeric network properties. RGD adhesive ligand and PEG-thiol were also conjugated to the polymer network, providing the microgels with excellent cell adhesive and visualization properties. Moreover, our PEG-4aNB microgels were crosslinked with the protease-degradable peptide VPM. Thus, the microgels could be easily degraded in presence of collagenase I (Figure 2c and d). For long-term periods of incubation in collagenase I (i.e. 5 days), faster degradation kinetics were observed for 6 and 8 wt% formulations compared to 10 wt%, which is likely due to the less dense polymer network of the lower polymer concentration microgels. These results show the ability to tune microgel properties with

this microfluidic approach. Recently, our group demonstrated that the *in vivo* degradation of norbornene-based PEG hydrogels can be tuned by changing the linkage groups within the thiol-ene PEG. We showed that by substituting the 4-arm ester-linked PEG-norbornene (PEG-4eNB) by an amide linkage (PEG-4aNB), the rapid degradation of PEG-4eNB could be mitigated and the *in vivo* stability of the PEG-NB hydrogels improved, providing a non-degradable *in vivo* platform for different applications.[7a] This work opened the door for the generation of PEG-NB biomaterials with more controllable degradation rates due to the photoconjugation of enzymatically degradable peptides in the polymer backbone, as shown in the current study. Thus, we present an attractive and facile approach to fabricated protease-sensitive degradable microgels that can be potentially applied for cell delivery applications. This approach offers several advantages when compared to previous reported degradable PEG-NB microgels, which showed an ultra-fast hydrolytic degradation upon contacting with aqueous solution,[4c] such us stimuli-dependent degradation, tunable degradation rate, and extended residence time for biomaterial engraftment when implanted.

Thiol-ene photocrosslinking reaction of PEG-NB has arisen as a suitable technique for 2D and 3D cell encapsulation and culture mainly due to the mild gelation conditions that occurs at physiological pH and the low concentration of free radicals generated during the photopolymerization process.[3a, 3c, 7a] Here, we demonstrate that hMSCs can be successfully encapsulated in PEG-4aNB microgels at 6, 8 and 10 wt% polymer concentration. Encapsulated cells showed excellent cell viability and metabolic activity for 13 days of culture, and even though no longer culture times where explored, these results demonstrate the potential of PEG-4aNB microgels as biomaterial platforms for long-term cell culture. Encapsulated hMSCs showed excellent cell morphology and spreading, colonizing the whole microgel surface at 15 days (Figure 3a). Cell viability was reduced after microgel encapsulation in comparison to pre-encapsulation viability (~84%). Several studies have demonstrated that even though photopolymerization is a mild and cytocompatible crosslinking mechanism, long-wave UV light (315–400 nm) can have detrimental effects on cell viability. However, these studies also demonstrated that UV light exposure did not induce significant changes in gene expression or differentiation capacity of MSCs, being able to maintain their functionality.[20] In our approach, relatively high cell viability during encapsulation process is favored due to mild conditions of thiol-ene photopolymerization, the high flow rates of the microgels in the microfluidic device that reduces the exposure time of the cells to UV light, and also to the relatively low UV irradiation intensity (32 mW/cm^2) necessary for the successful crosslinking of the hydrogel microparticles in comparison to other UV-light mediated encapsulation protocols that apply UV irradiation intensities up to 100 mW/cm^2.[3c] We posit that the decreased cell viability after encapsulation is impacted by the washing steps when cells remain without media for a short period of time. Cell metabolic activity showed significantly higher metabolic activity, inferred to reflect cell proliferation, over time for every microgel composition. hMSCs encapsulated in 8 and 10 wt% PEG-4aNB microgels demonstrated significantly higher metabolic activity at 13 days of culture in comparison to 6 wt% microgel formulation. These results support the conclusion that PEG-4aNB microgels provide a suitable microenvironment with high cytocompatibility for cell encapsulation

and cell carrier applications, which are critical parameters for therapeutic cell delivery applications together with sustained cell viability after photoencapsulation process.

hMSCs have attracted a deep therapeutic interest as a promising cell source for the treatment of degenerative and inflammatory diseases.[11, 21] Although this interest was first focused in the ability of hMSCs to differentiate into different cell lineages and their self-renewal capacity, investigations have attributed hMSC therapeutic effects to paracrine signaling via the secretion of bioactive factors that influence tissue remodeling processes and trigger immunomodulatory responses.[12, 22] We analyzed the secretome profile of hMSCs encapsulated in PEG-4aNB microgels for 23 different analytes. Our results showed that the analytes were upregulated in the presence of the stimulating factor IFN-γ. Individual analysis of secreted analytes demonstrated that the encapsulated hMSCs in 10 wt% PEG-4aNB microgels showed generally significant higher secretion of the analytes that were upregulated upon IFN-γ stimulation when compared to the other two PEG-4aNB formulations. These results correlate well with the significant higher metabolic activity found for encapsulated hMSCs in 10 wt% microgel formulation. Among analytes with increased expression for hMSCs encapsulated in PEG-4aNB microgels, CXCL9 and PD-L1 are of particular interest.[18, 23] CXCL9 chemokine has been identified to play a key immune checkpoint inhibition in preclinical cancer models, [18a] together with other two family members, CXCL10 and CXCL11, and arising as a target for novel cancer therapy.[18, 23a] CXCL9 induces PD-L1 expression via CXCR3 signaling cascade.[23a] Other upregulated analytes in encapsulated hMSCs are related to immune responses and T-cell recruitment processes (i.e., IL-6, IL-12, IL-17E). Overall, these results show that the stimulation of encapsulated hMSCs with IFN-γ triggered the expression of analytes related to immune-related, indicating the immunoregulatory potential and functionality of the encapsulated cells in PEG-4aNB microgels.

5. Conclusion

We present a rapid and facile approach to synthesize protease-degradable PEG-4aNB microgels with high uniformity and well-controlled size. The mild crosslinking conditions and microfluidic set-up permit the encapsulation of hMSCs with excellent viability and metabolic activity after encapsulation, which was sustained over time. Finally, the secretory profile of the encapsulated hMSCs showed increased expression in presence of IFN-γ. Cytokine upregulation was increased in hMSCs encapsulated in 10 wt% microgels. Overall, these results indicated the suitability of PEG-4aNB microgels cell carrier platforms. We envision that this synthesis approach will make a huge impact on the cell encapsulation field for more sensitive cell lines.

Supplementary Material

Refer to Web version on PubMed Central for supplementary material.

Acknowledgements

Research was in part funded by the U.S. National Institutes of Health (R01 AR062368) and European Research Executive Agency under Individual GLOBAL Marie Skłodowska-Curie Actions Fellowship (project n° 101028216

— SYNMAT FOR ORGANOIDS). S.G.G. was beneficiary of a Petit Scholar grant by NSF Engineering Research Center for Cell Manufacturing Technologies (CMaT). hMSCs were obtained from the Texas A&M Health Science Center College of Medicine Institute for Regenerative Medicine at Scott & White through a grant from ORIP of the NIH (P40OD011050). Finally, A.M.B acknowledges her gratitude and respects to Dr. Blanca Vazquez-Lasa, who was a dedicated researcher at the Institute of Polymer Science and Technology (ICTP-CSIC, Spain), working with natural polymers and their applications in regenerative medicine. Dr. Blanca Vazquez-Lasa spent her life mentoring young researchers with passion and kindness, being a role model for many of her students.

References

[1]. a)Headen DM, Aubry G, Lu H, Garcia AJ, Adv Mater 2014, 26, 3003; [PubMed: 24615922] b)Daly AC, Riley L, Segura T, Burdick JA, Nat Rev Mater 2020, 5, 20; [PubMed: 34123409] c)Xu Y, Zhu H, Denduluri A, Ou Y, Erkamp NA, Qi R, Shen Y, Knowles TPJ, Small 2022, 18, 2200180.

[2]. a)Headen DM, García JR, García AJ, Microsystems & Nanoengineering 2018, 4, 17076;b)Coronel MM, Martin KE, Hunckler MD, Kalelkar P, Shah RM, Garcia AJ, Small 2022, 18, e2106896; [PubMed: 35274457] c)Lin C-C, Ki CS, Shih H, Journal of Applied Polymer Science 2015, 132.

[3]. a)Lin CC, Ki CS, Shih H, J Appl Polym Sci 2015, 132;b)Fraser AK, Ki CS, Lin C-C, Macromolecular Chemistry and Physics 2014, 215, 507;c)Jiang Z, Xia B, McBride R, Oakey J, J Mater Chem B 2017, 5, 173. [PubMed: 28066550]

[4]. a)Xin S, Chimene D, Garza JE, Gaharwar AK, Alge DL, Biomaterials Science 2019, 7, 1179; [PubMed: 30656307] b)Xin S, Wyman OM, Alge DL, Adv Healthc Mater 2018, 7, e1800160; [PubMed: 29663702] c)Jiang Z, Lin F-Y, Jiang K, Nguyen H, Chang C-Y, Lin C-C, Biomaterials Advances 2022, 134, 112712; [PubMed: 35581097] d)Gregoritza M, Abstiens K, Graf M, Goepferich AM, Eur J Pharm Biopharm 2018, 127, 194; [PubMed: 29471077] e)Emiroglu DB, Bekcic A, Dranseikiene D, Zhang X, Zambelli T, deMello AJ, Tibbitt MW, Science Advances 2022, 8, eadd8570. [PubMed: 36525484]

[5]. a)Foster GA, Headen DM, González-García C, Salmerón-Sánchez M, Shirwan H, García AJ, Biomaterials 2017, 113, 170; [PubMed: 27816000] b)Jiang Z, Shaha R, McBride R, Jiang K, Tang M, Xu B, Goroncy AK, Frick C, Oakey J, Biofabrication 2020, 12, 035006. [PubMed: 32160605]

[6]. a); b)Jalili-Firoozinezhad S, Gazzaniga FS, Calamari EL, Camacho DM, Fadel CW, Bein A, Swenor B, Nestor B, Cronce MJ, Tovaglieri A, Levy O, Gregory KE, Breault DT, Cabral JMS, Kasper DL, Novak R, Ingber DE, Nat Biomed Eng 2019, 3, 520; [PubMed: 31086325] c)Li F, Truong VX, Thissen H, Frith JE, Forsythe JS, ACS Applied Materials & Interfaces 2017, 9, 8589. [PubMed: 28225583]

[7]. a)Hunckler MD, Medina JD, Coronel MM, Weaver JD, Stabler CL, Garcia AJ, Adv Healthc Mater 2019, 8, e1900371; [PubMed: 31111689] b)Lin F-Y, Lin C-C, ACS Macro Letters 2021, 10, 341. [PubMed: 35549061]

[8]. a)Koh J, Griffin DR, Archang MM, Feng AC, Horn T, Margolis M, Zalazar D, Segura T, Scumpia PO, Di Carlo D, Small 2019, 15, e1903147; [PubMed: 31410986] b)Griffin DR, Weaver WM, Scumpia PO, Di Carlo D, Segura T, Nat Mater 2015, 14, 737; [PubMed: 26030305] c)Flégeau K, Puiggali-Jou A, Zenobi-Wong M, Biofabrication 2022, 14, 034105.

[9]. Eun YJ, Utada AS, Copeland MF, Takeuchi S, Weibel DB, ACS Chem Biol 2011, 6, 260. [PubMed: 21142208]

[10]. a)Matsukawa S, Brenner T, Nano/Micro Science and Technology in Biorheology: Principles, Methods, and Applications 2015, 129;b)Callaghan PT, Translational dynamics and magnetic resonance : principles of pulsed gradient spin echo NMR, Oxford ; New York : Oxford University Press, 2011., 2011.

[11]. Schneider RS, Vela AC, Williams EK, Martin KE, Lam WA, Garcia AJ, Adv Healthc Mater 2022, 11, e2101995. [PubMed: 34725948]

[12]. a)Daniel Ascencio G, Rogelio Hernández P, Miguel Ángel Gómez L, Sergio Ayala F, Aaron Torres G, in Stromal Cells, (Ed: Mani TV), IntechOpen, Rijeka 2018;b)Gnecchi M, Ciuffreda MC, Mura M, in Cell Engineering and Regeneration, (Eds: Gimble JM, Marolt D, Oreffo R, Redl H, Wolbank S), Springer International Publishing, Cham 2019.

[13]. Galipeau J, Krampera M, Barrett J, Dazzi F, Deans RJ, DeBruijn J, Dominici M, Fibbe WE, Gee AP, Gimble JM, Hematti P, Koh MB, LeBlanc K, Martin I, McNiece IK, Mendicino M, Oh S, Ortiz L, Phinney DG, Planat V, Shi Y, Stroncek DF, Viswanathan S, Weiss DJ, Sensebe L, Cytotherapy 2016, 18, 151. [PubMed: 26724220]

[14]. Hu Q, Ecker M, Int J Mol Sci 2021, 22. [PubMed: 35008458]

[15]. Bui TM, Wiesolek HL, Sumagin R, J Leukoc Biol 2020, 108, 787. [PubMed: 32182390]

[16]. Hasegawa H, Mizoguchi I, Chiba Y, Ohashi M, Xu M, Yoshimoto T, Frontiers in Immunology 2016, 7.

[17]. Borowczyk J, Shutova M, Brembilla NC, Boehncke WH, J Allergy Clin Immunol 2021, 148, 40. [PubMed: 33485651]

[18]. a)Seitz S, Dreyer TF, Stange C, Steiger K, Bräuer R, Scheutz L, Multhoff G, Weichert W, Kiechle M, Magdolen V, Bronger H, British Journal of Cancer 2022, 126, 1470; [PubMed: 35314795] b)Zhang C, Li Z, Xu L, Che X, Wen T, Fan Y, Li C, Wang S, Cheng Y, Wang X, Qu X, Liu Y, BMC Cancer 2018, 18.

[19]. Baret J-C, Lab on a Chip 2012, 12, 422. [PubMed: 22011791]

[20]. a)Wong DY, Ranganath T, Kasko AM, PLoS One 2015, 10, e0139307; [PubMed: 26418040] b)Fedorovich NE, Oudshoorn MH, van Geemen D, Hennink WE, Alblas J, Dhert WJA, Biomaterials 2009, 30, 344. [PubMed: 18930540]

[21]. Pittenger MF, Discher DE, Péault BM, Phinney DG, Hare JM, Caplan AI, npj Regenerative Medicine 2019, 4, 22. [PubMed: 31815001]

[22]. Mora-Boza A, Mancipe Castro LM, Schneider RS, Han WM, Garcia AJ, Vazquez-Lasa B, San Roman J, Mater Sci Eng C Mater Biol Appl 2021, 120, 111716. [PubMed: 33545868]

[23]. a)Xiu W, Luo J, BMC Immunology 2021, 22, 3; [PubMed: 33407095] b)Lotfy A, Wang H, Stem Cell Reviews and Reports 2022.

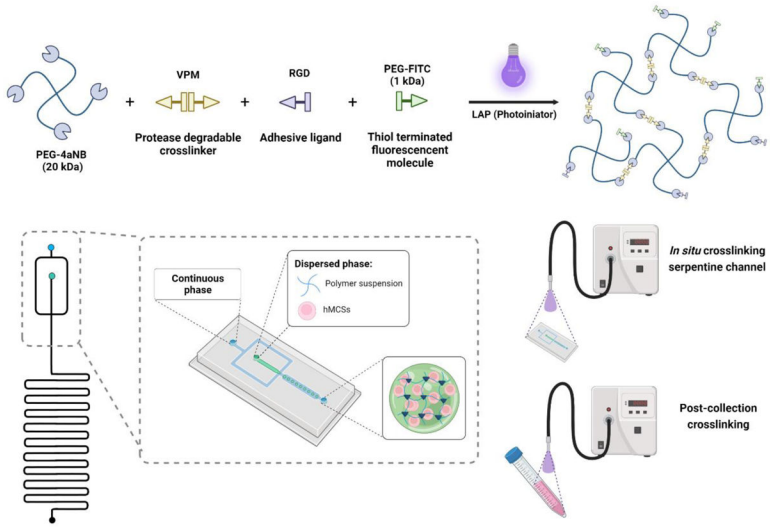

Figure 1:

PEG-4aNB crosslinking strategy for microgel synthesis using microfluidics. a) Photopolymerization reaction of PEG-4aNB functionalized with RGD and thiol-PEG-FITC using VPM as protease degradable crosslinking agent and LAP as photoinitiator. b) Schematic of microfluidic device used PEG-4aNB microgels preparation. Microgels were crosslinked in the device by applying UV light directly to the microfluidic device (*in situ* crosslinking) or after collection (post-collection crosslinking).

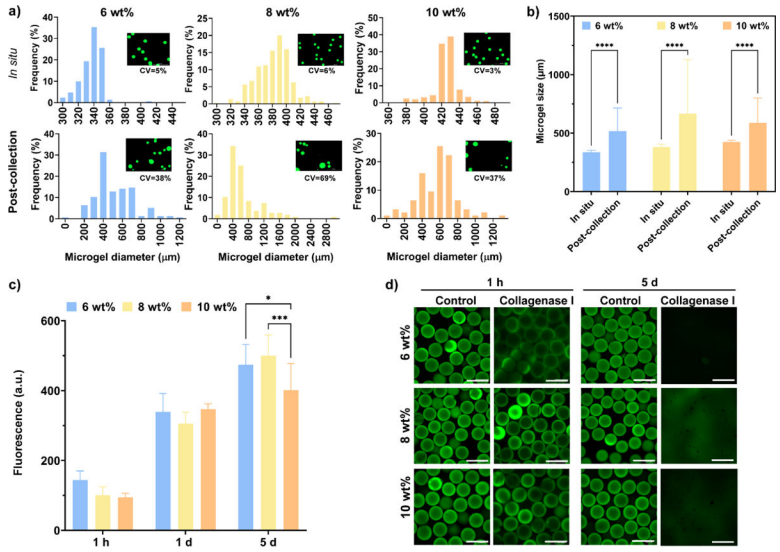

Figure 2:

PEG-4aNB microgel size distributions and proteolytic degradation kinetics. a) Size distribution histograms for 6, 8, and 10 wt% microgels for *in situ* crosslinked and post-collection crosslinked microgels approaches, accompanied by fluorescence images of each microgel group after purification and values for coefficient of variation (%CV). b) PEG-4aNB microgel diameter values for 6, 8, and 10 wt% polymer concentration for *in situ* and post-collection approaches (mean ± SD). c) Tracking of released PEG-FITC in solution over time for 6, 8 and 10 wt% PEG-4aNB microgels in presence of 3.9 units/mL collagenase I. d) Fluorescence images for 6, 8, and 10 wt% PEG-4aNB microgels in PBS as control and in 3.9 units/mL collagenase I after 1 hour and 5 days of incubation; *p<0.01, ***p=0.0005, ****p<0.0001. Two-way ANOVA analysis was used to detect significant differences among samples.

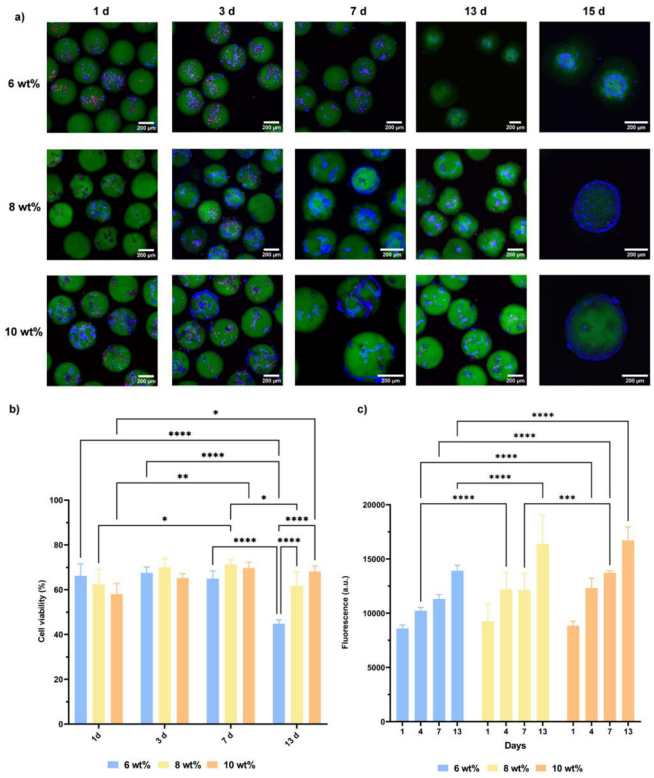

Figure 3:

Cell viability and metabolic activity of encapsulated hMSCs in 6, 8 and 10 wt% PEG-4aNB microgels over time. a) Confocal images of Live/Dead staining after 1, 3, 7, 13 and 15 days of culture. Live cells are shown in blue (LIVE 405 dye), dead cells in red (TOTO-3 dye) and microgels in green (PEG-FTIC). b) Cell viability analysis for encapsulated hMSCs in 6, 8 and 10 wt% PEG-4aNB microgels after 1, 3, 7 and 13 days of culture. c) Metabolic activity analyzed by alamarBlue assay of encapsulated hMSCs in PEG-4aNB microgels after 1, 3, 7 and 13 days of culture. n = 4 biologically independent samples, mean ± SD; *p < 0.01, **p < 0.001, ***p = 0.0002, ****p < 0.0001. Two-way ANOVA analysis was used to test for differences among groups.

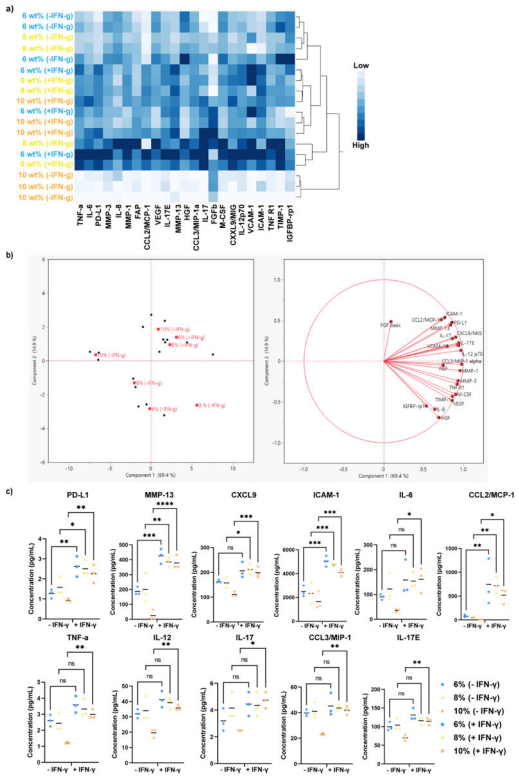

Figure 4:

Cytokine secretion of encapsulated hMSCs in 6, 8 and 10 wt% PEG-4aNB microgels in the absence and presence of IFN-γ. A) Heat map and two-way hierarchal clustering of analyte secretion. b) Principal components analysis (PCA) for analytes secretion. c) Individual analysis of factors secreted from encapsulated hMSCs in 6, 8 and 10 wt% PEG-4aNB microgels; n = 3 biologically independent samples, mean ± SD; *p < 0.05, **p < 0.01, ***p < 0.001, ****p<0.0001. One-way ANOVA analysis was used to detect differences among samples.